

Short communication

Aircraft measurements of the vertical distribution of sulfur dioxide and aerosol scattering coefficient in China

Likun Xue^{a,b}, Aijun Ding^{b,1}, Jian Gao^{a,b,2}, Tao Wang^{a,b,c,*}, Wenxing Wang^a, Xuezhong Wang^c, Hengchi Lei^d, Dezhen Jin^e, Yanbin Qi^e^a Environment Research Institute, Shandong University, Ji'nan, Shandong, PR China^b Department of Civil and Structural Engineering, The Hong Kong Polytechnic University, Hong Kong, PR China^c Chinese Research Academy of Environmental Sciences, Beijing, PR China^d Institute of Atmospheric Physics, Chinese Academy of Sciences, Beijing, PR China^e Weather Modification Office, Jilin Provincial Meteorological Bureau, Changchun, PR China

ARTICLE INFO

Article history:

Received 20 June 2009

Received in revised form

13 October 2009

Accepted 15 October 2009

Keywords:

Aircraft observation

Vertical profile

SO₂

PBL

OMI retrieval

ABSTRACT

Information on the vertical distribution of air pollution is important for understanding its sources and processes and validating satellite retrievals and chemical transport models. This paper reports the results of the measurements of sulfur dioxide (SO₂) and aerosol scattering coefficient (B_{sp}) obtained from several aircraft campaigns during summer and autumn 2007 in the north-eastern (NE), north-western (NW), and central-eastern (CE) regions of China. Their vertical profiles over the three regions with contrasting emission characteristics and climates are compared. Very high concentrations/values of SO₂ and B_{sp} (with a value of up to 51 ppbv and 950 Mm⁻¹, respectively) were recorded in the lower planetary boundary layer in CE China, indicating high SO₂ emissions in the region. The SO₂ column concentrations determined from the in-situ measurements were compared with Ozone Monitoring Instrument (OMI) SO₂ retrievals. The results show that the OMI data could distinguish the varying levels of SO₂ pollution in the study regions, but appeared to have underestimated the SO₂ column in the highly polluted region of CE China.

© 2009 Elsevier Ltd. All rights reserved.

1. Introduction

Sulfur dioxide (SO₂) is an important trace gas in the atmosphere. At high concentrations it has a direct negative effect on human health (Ware et al., 1981); through the formation of acid rain, it damages forests and acidifies aquatic systems (Likens et al., 1972). Sulfate particles formed from the oxidation of SO₂ reduce visibility and change the climate directly by scattering sunlight and indirectly by affecting cloud optical properties (Penner et al., 1998; IPCC, 2007). SO₂ emissions in North America and Europe have decreased significantly since the 1980s (Smith et al., 2001; Vestreng et al., 2007), whereas in China, they have increased by 200–300% over the past three decades because of the dramatic increase in the consumption of coal due to rapid industrialization (Ohara et al., 2007; Li and

Oberheitmann, 2009). Many cities in northern China suffer from high levels of SO₂ and sulfate particles, while southern China experiences persistent acidic rainfall (e.g., Wang and Wang, 1996; Hao and Wang, 2005; Chan and Yao, 2008).

Of the great number of studies of SO₂, sulfate, and optical properties (see Chan and Yao, 2008), only a few provide information on the vertical profiles in the troposphere (Wang et al., 2005; Dickerson et al., 2007). In view of the importance of such data in understanding vertical exchange/transport processes and evaluating satellite retrieval algorithms and chemical transport models, we carried out several aircraft measurement campaigns in three regions of China, including the northeast (NE), which is China's major agricultural base, the northwest (NW), which is sparsely populated and has an arid and semi-arid climate, and the central-eastern (CE) region, which is the largest flat area and thus the most populated and heavily industrialized region of China. This paper presents the overall characteristics of the vertical profiles of SO₂ and aerosol scattering coefficients (B_{sp}) and compares, in a preliminary fashion, in-situ measured and satellite-derived SO₂ columns over the three regions. A detailed analysis of a case of photochemical pollution observed on a flight in NE China has been presented in Ding et al. (2009).

* Corresponding author at: Department of Civil and Structural Engineering, The Hong Kong Polytechnic University, Hong Kong, PR China. Tel.: +852 2766 6059; fax: +852 2334 6389.

E-mail address: cetwang@polyu.edu.hk (T. Wang).

¹ Now at School of Atmospheric Sciences, Nanjing University, Nanjing, PR China.

² Now at Chinese Research Academy of Environmental Sciences, Beijing, PR China.

2. Description of the experiment

2.1. Study region

Three campaigns were conducted from June to October in 2007 over a large portion of China (see Fig. 1). In NE China, 16 flights were conducted from June 20 to July 13, over Changchun, the capital of Jilin province. The aircraft took off from an airport (125.2° E, 43.9° N, ~245 m ASL) located in the northwest of the city. A majority of flights were carried out around noon, with a mean spiral time of 11:15 LT (± 4 h). An examination of global reanalysis data (figures not shown) suggests that during the study period, NE China was influenced by a low pressure system and the planetary boundary layer (PBL) air mostly came from the ocean in the south and from CE China in the southwest. In NW China, seven flights were carried out in August 2007 in Gansu province, which is a region with complex terrain and a dry climate with much fewer anthropogenic sources, except for an isolated large source of Lanzhou city. Our aircraft flew off Zhongchuan airport (103.6° E, 36.5° N, ~1860 m ASL), about 50 km northwest of Lanzhou (mean time 11:40 LT ± 2.5 h). During August, the lower tropospheric air generally came from central China from the east. During September and October 2007, four flights were conducted from Ji'nan Yaoqiang airport (117.2° E, 36.9° N, ~20 m ASL), about 30 km northeast of Ji'nan city in Shandong province, with mean spiral time at 13:45 LT (± 3 h); in addition, three flights were made over Wuxi (120.3° E, 31.6° N, ~10 m ASL) in the neighboring Jiangsu province (mean spiral time 13:00 LT ± 3 h). Shandong is the largest emitter of SO₂ among China's 31 provinces and municipalities. During the measurement period, the region was under the strong influence of a sub-tropical high with weak north winds in the PBL, which created conditions favorable to the accumulation of air pollution.

2.2. Instrumentation

A twin-engine turboprop Yun-12 aircraft, similar to a Twin Otter, served as the sampling platform in these studies. The aircraft has a typical speed of 240 km h⁻¹ and a maximum flight range of about 1340 km, with a ceiling altitude of 7000 m. The sampling inlet was mounted at the bottom of the aircraft, inside which an aft-facing inlet connected with the gas analyzers while an isokinetic forward-facing inlet fed the aerosol instruments. SO₂ was measured using a pulsed UV fluorescence analyzer (TEI, Model 43C TL) with

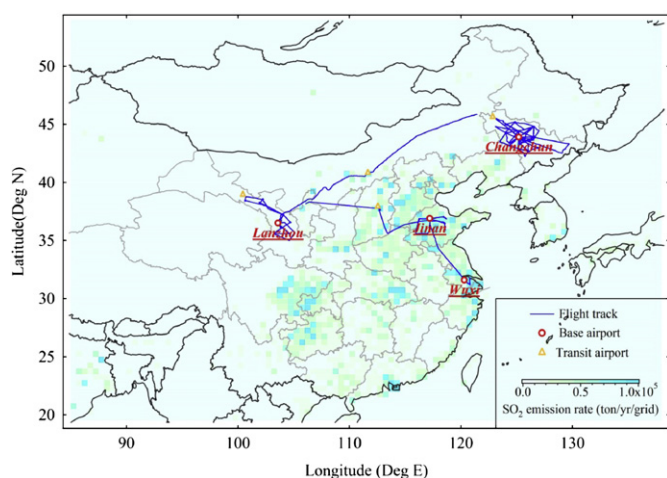


Fig. 1. Map showing flight tracks and anthropogenic SO₂ emission rates over China. Emission data were obtained from http://www.cgrrer.uiowa.edu/EMISSION_DATA_new/index_16.html.

a detection limit of 0.20 ppbv for 10-s integration and a precision of about 0.10 ppbv. Aerosol scattering coefficients were measured with an integrating nephelometer (EcoTech, M9003), which detects light scattering coefficients (B_{sp}) at 520 nm with a detection limit of $<0.3 \text{ Mm}^{-1}$ for 1-min integration and a light scattering angle of 10–170°. Calibrations were performed regularly on the ground and also on board during several flights. A data logger (Environmental System Corporation, Model 8816) was used to collect 5-s averaged data of SO₂, which represents a horizontal resolution of ~350 m or a vertical scale of ~20 m. In addition, air temperature, pressure, relative humidity (RH), liquid water content (LWC; measured using the on board forward scattering spectrometer probe FSSP-100, PMS Inc.), and global positioning system (GPS) data were also recorded during the flights. Temperature and pressure were available for only Changchun and Ji'nan.

In the present work, we focus on the vertical profiles of SO₂ and B_{sp} recorded in the ascent and descent stages over Changchun, Lanzhou, Ji'nan, and Wuxi. Note that B_{sp} was not measured over Wuxi. Each spiral typically lasted 10–30 min. All of the measurements used here were confined within a domain of $1^\circ \times 1^\circ$ centered at the airports and within an altitude range from the surface to about 3 km (2 km for Ji'nan).

3. Results

3.1. Vertical profiles and intercorrelations

Fig. 2a shows the mean vertical profiles of SO₂ over Changchun, Lanzhou, Ji'nan, and Wuxi, with each point representing the mean concentration in a 300-m bin. Because all of the flights were over suburban/rural areas, the profiles are thought to be representative of the four regions. The figure shows that all of the profiles have a broader peak near the surface, which decreases with altitude. This is typical and can be explained by the interplay between surface emissions, turbulence mixing, and the dry deposition of SO₂. Moderate levels of SO₂ (4–6 ppbv) were observed over NE and NW China (i.e., Changchun and Lanzhou), but an extremely high SO₂ concentration existed in the PBL of CE China (i.e., Wuxi and Ji'nan), especially Ji'nan, where a mean value of up to 51 ppbv was observed in the lowest part of the atmosphere. Fig. 2a also shows that the mixing ratios of SO₂ were invariant with height in the free troposphere (altitude > 1.5 km). The free tropospheric concentrations (0.5–3.0 ppbv), especially in eastern China, were much higher than those observed in continental Europe and the United States (Preunkert et al., 2007; Hains et al., 2008). The elevated SO₂ concentration in the free troposphere may be due to PBL/free troposphere exchange processes, such as warm conveyor belts and convection in warm seasons (Wild and Akimoto, 2001; Ding et al., 2009).

B_{sp} levels in NW and NE China (see Fig. 2b) were slightly larger than those observed in North America and western Europe (Guibert et al., 2005; Hains et al., 2008), while that of Ji'nan was 5–10 times higher, indicating the presence of high concentrations of particulate matter in the PBL of the North China Plain. Integrating B_{sp} in the lower troposphere gave an aerosol optical thickness (assuming a constant SSA of 0.9) of 0.42, 0.25, and 1.24 for Changchun, Lanzhou, and Ji'nan, respectively (see also Table 1). B_{sp} shows almost a linear decrease with altitude, in contrast to the more gradual decrease of SO₂ in the PBL and sharper decline in the free troposphere. This difference is likely due to the larger dry deposition velocity of SO₂ compared to that of fine aerosol (Xu and Carmichael, 1998). Although Changchun and Lanzhou had comparable SO₂ concentrations, the former had a higher B_{sp} concentration, which can be explained by the large aerosol loading and/or higher relative humidity in NE China.

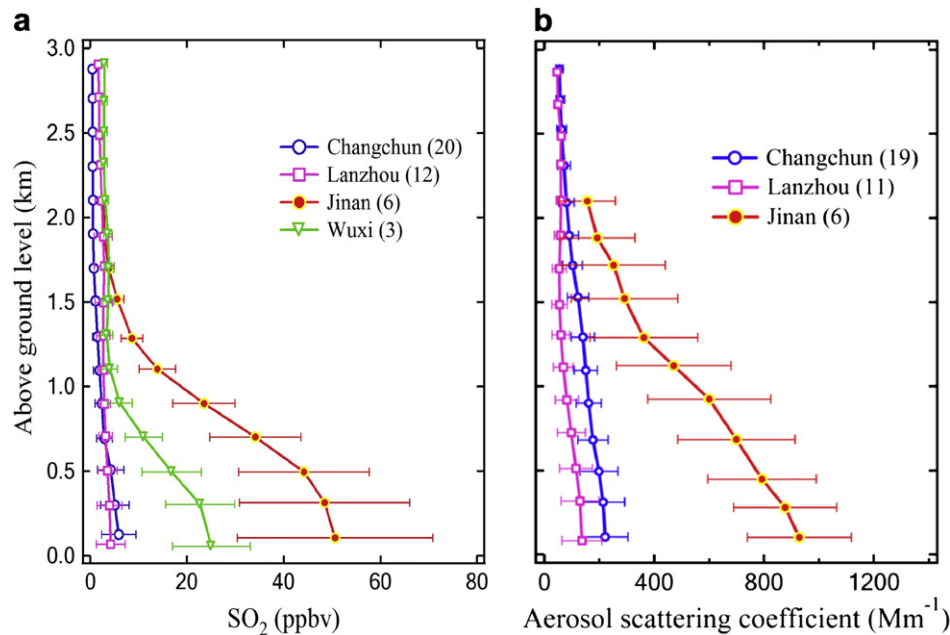


Fig. 2. Mean vertical profiles of (a) SO_2 and (b) B_{sp} over Changchun, Lanzhou, Ji'nan, and Wuxi. Solid bars represent half of the standard deviation for data points in 300-m bins. The number of profiles for each location is given in parentheses.

Fig. 2 shows the averaged vertical profiles. Individual case could be quite different from the mean profiles due to the variation in dynamic and transport processes. For example, we observed a layer of highly polluted air in the free troposphere over Jilin on 27 June, which was attributed to the transport associated with the warm conveyor belts (Ding et al., 2009). At Lanzhou, we also observed elevated SO_2 and B_{sp} values above the PBL, which was possibly due to the topographical lifting in that region.

Oxidation of SO_2 leads to the formation of sulfate aerosol, which is one of the principal contributors to particle scattering (Seinfeld and Pandis, 2006). It is of interest therefore to examine the relationship between SO_2 and B_{sp} . The scattering ability of sulfate aerosol depends not only on its mass but also RH because of its ability to absorb water vapor. Here we use the $f(\text{RH})$ functions from Malm and Day (2001) to calculate aerosol scattering coefficients ($B_{\text{sp,dry}}$) at dry conditions ($\text{RH} < 20\%$). The $f(\text{RH})$ measured from Great Smoky (cf. Table 3 in Malm and Day, 2001) was applied to the data from Changchun and Ji'nan, whereas that of Great Canyon (cf. Table 4) was chosen for Lanzhou because of the similar dry climate and a small fraction of inorganic ions in $\text{PM}_{2.5}$ at Lanzhou (Pathak et al., 2009) and at Great Canyon. Fig. 3a presents the scatter plots of $B_{\text{sp,dry}}$ vs. SO_2 in three altitude bands over Changchun. It shows that the $B_{\text{sp,dry}}/\text{SO}_2$ ratio increased with altitude (from 8 to 30), indicating a more aged air mass at higher altitudes. Fig. 3b and c shows the results for Lanzhou and Ji'nan, respectively

(Note the enlarged scales in Fig. 3c). Those of Lanzhou are quite scattered, but those of Ji'nan show an altitude-dependence similar to that of Changchun. The much greater aerosol scattering (and by inference, poor visibility) in CE China reflects the high anthropogenic emissions of SO_2 and other pollutants in the region.

3.2. Comparison with OMI SO_2 data

One of the unique uses of aircraft vertical profiles is to evaluate/improve satellite retrievals. In this section, we compare the aircraft measurements with OMI (Ozone Monitoring Instrument) SO_2 products from PBL SO_2 column retrievals (column amount $\text{SO}_2\text{-PBL}$), which are processed with a band residual difference (BRD) algorithm (Krotkov et al., 2006). Considering the data sensitivity and possible uncertainty related to cloud and other factors, for the target locations we selected only the OMI data within the $1^\circ \times 1^\circ$ grid, following the criteria of cloud fraction < 0.2 , solar zenith angle $< 60^\circ$ and near-nadir viewing angles (cross-track positions 20–40) (Dr. N.A. Krotkov, personal communication). We integrated the aircraft profiles to estimate the SO_2 columns over the spiral regions. Temperature and pressure corrections were made with our measurements or with the default profiles of the U.S. Standard Atmosphere for the missing data at Lanzhou. We estimate that the bias from the use of the standard atmosphere was small (< 0.1 DU for a variation of 100 hPa and 10 K). The mean SO_2

Table 1
Comparison of mean SO_2 columns derived from aircraft in-situ profiles and OMI satellite retrievals.

Location	Period	Aircraft			OMI Satellite		
		Number of profiles	SO_2 Column ^a DU	AOT ^b	Number of valid days ^c	SO_2 column DU	Slant column ozone ^d DU
Changchun (124.7 E – 125.7 E, 43.5 N – 44.5 N)	Jun 20 – Jul 20	(20)	0.58 (0.36)	0.42	(8)	0.52 (0.93)	724 (31)
Lanzhou (103.5 E – 104.5 E, 36 N – 37 N)	Jul 31 – Aug 31	(12)	0.64 (0.48)	0.25	(6)	0.98 (0.55)	602 (14)
Ji'nan (117 E – 118 E, 36 N – 37 N)	October	(6)	4.39 (2.04)	1.24	(6)	2.88 (2.04)	738 (70)

^a Extrapolated from the surface to 3 km (0–2 km for Ji'nan).

^b Estimated from the aircraft mean altitude profile of B_{sp} assuming a constant SSA of 0.9.

^c The operational OMI SO_2 data with optimal viewing conditions (radioactive cloud fraction < 0.2 , solar zenith angle $< 60^\circ$, cross-track position 20–40).

^d SCO is to account for the AMF errors from both observational geometry and total ozone (Ω). $\text{SCO} = \Omega \cdot (\sec(\text{SZA}) + \sec(\text{VZA}))$ [http://so2.umbc.edu/omi/].

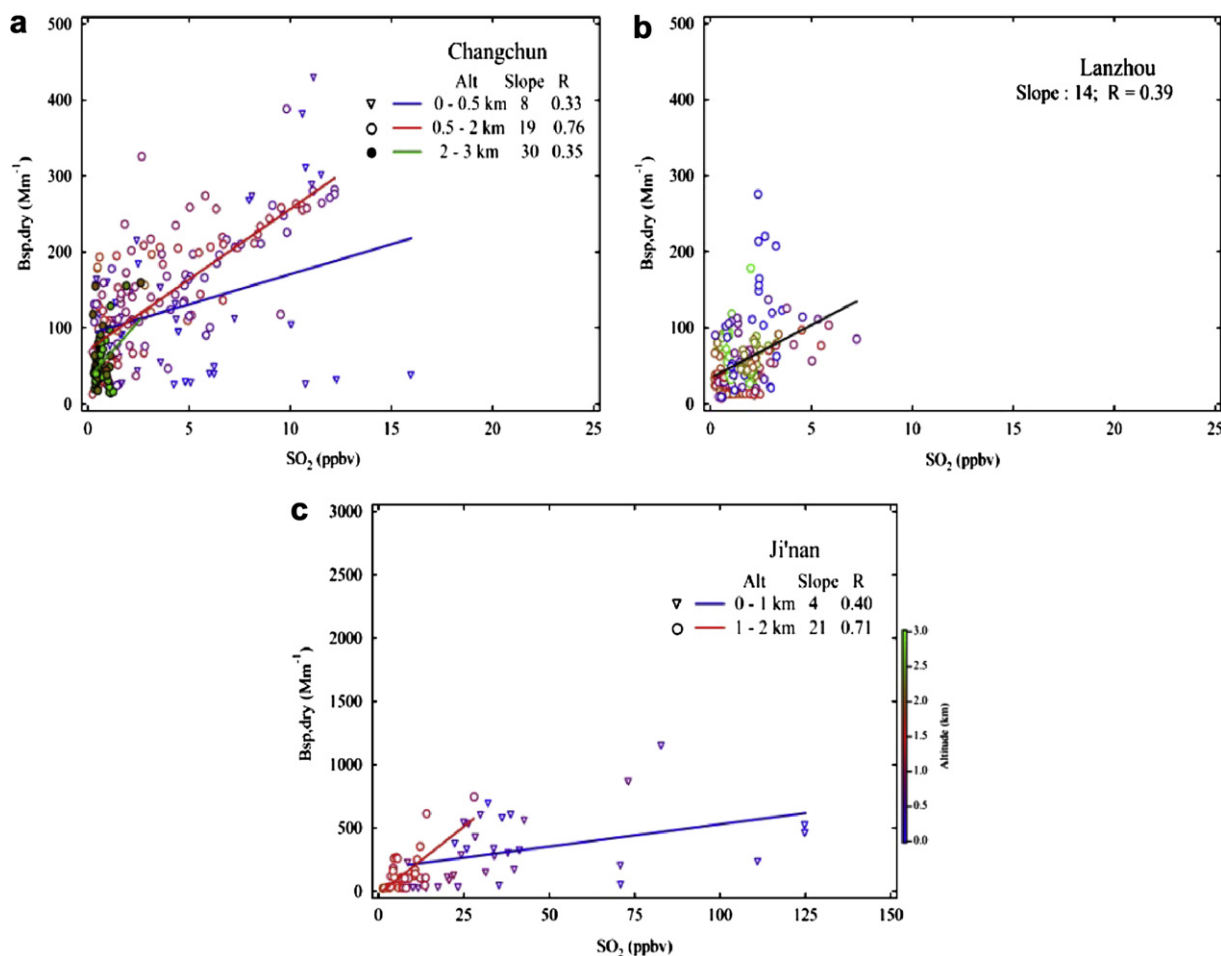


Fig. 3. Correlations between $B_{sp,dry}$ and SO_2 for three altitude bands over (a) Changchun and (b) Lanzhou and two altitude bands over (c) Ji'nan. All of the symbols are color coded with the flight altitude. Note that scales of (c) are enlarged by an equal proportion in order to show the high concentrations of SO_2 and B_{sp} in Ji'nan.

columns from OMI and aircraft are shown in Table 1 for Changchun, Lanzhou, and Ji'nan. The results suggest that OMI could distinguish different levels of anthropogenic SO_2 in the three regions; however, in the highly polluted North China Plain where Ji'nan is located, the OMI-retrieved SO_2 column was much lower than the aircraft result (2.88 Dobson Units [DU] compared with 4.39 DU, respectively).

Surface albedo, cloud cover, the SO_2 empirical profile, slant column ozone (SCO), aerosol loading, and optical properties (i.e., single scattering albedo) can affect SO_2 retrieval (Carn et al., 2007; Krotkov et al., 2008). To investigate the possible reasons for the underestimation of the satellite retrievals in the Ji'nan area, we examine one flight at 13:40 LT on October 25, which was close to the time of the satellite overpass ($\sim 13:18$ LT). In this case, very high concentrations of SO_2 (>80 ppbv at 300 m and ~ 10 ppbv at 1600 m) were recorded during the ascent stage (figures not given). The aircraft-measured SO_2 column was 7 DU, integrating SO_2 the surface to 2 km (the highest altitude on that flight). The mean OMI SO_2 column was 5.35 DU obtained from a domain of $20\text{ km} \times 20\text{ km}$ over the region of spiral (only one IFOV data with the solar zenith angle of about 53° and the cross-track position of about 20). An examination of the satellite cloud map suggests that there was little cloud cover on that day (cloud fraction: ~ 0.18). The aircraft-measured SO_2 profile was quite similar to the default profile in the OMI retrieval algorithm (OMSO₂ README File, <http://so2.umbc.edu/omi/>). Thus, the uncertainties from these two factors would be very small. Regarding the SCO of 799 DU, we estimate that it

could have underestimated the SO_2 column by no more than 4% (Krotkov et al., 2008). It has been suggested that ultraviolet (UV) absorption by mineral dust and black carbon can significantly reduce the air mass factor (AMF) in the algorithms (Colarco et al., 2002; Torres et al., 2007; Krotkov et al., 2008). Although unpublished data obtained by researchers of Shandong University in Ji'nan urban area indicate absorbing nature of aerosols (with single scattering albedo of ~ 0.80), no data are available outside the city where the aircraft measurement took place. The OMI UV Aerosol Index (AI) on Oct 25 was 1.07. It does not provide definitive information on absorbing or scattering nature of aerosols in the planetary boundary layer, as previous research mainly used the AI to show the abundance of absorbing aerosol at high altitudes (i.e., in dust and biomass burning plumes), and the sensitivity of AI decreases at lower altitudes (Ahn et al., 2008). It is possible that the smaller value of OMI SO_2 column may be due to absorbing aerosol in the Ji'nan region, but data on the optical properties of aerosol are needed to confirm this contention.

4. Summary

The vertical profiles of SO_2 and aerosol scattering coefficients were measured in 2007 on board an aircraft in the north-eastern, north-western, and central-eastern parts of China. These regions have different air pollution levels and climates. The results revealed very high concentrations of SO_2 and B_{sp} in the plains of central-eastern

China, especially in Shandong, where an averaged PBL SO₂ of up to 51 ppbv was observed. A better correlation between B_{sp,dry} and SO₂ and larger B_{sp,dry}/SO₂ ratios were found at higher altitudes. Comparison of the aircraft-measured and OMI-derived SO₂ columns suggests that OMI SO₂ retrieval could distinguish different pollution levels of anthropogenic SO₂ in the three study regions, but may have underestimated the SO₂ column in the highly polluted Ji'nan area. It is possible that UV-absorbing aerosols (black carbon) were present over the Ji'nan region which caused the underestimation. More aircraft studies in central-eastern China are needed to verify the results of this work, which are based on a limited number of flights.

Acknowledgements

The authors would like to thank Jilin Provincial Meteorological Bureau, Gansu Provincial Meteorological Bureau, and Shandong Provincial Meteorological Bureau for their cooperation and support during the aircraft campaigns. We thank Steven Poon and Xiaoqing Zhang for mounting the aircraft instruments. We are grateful to the aircraft crew members, especially Colonel Kuilin Li, for their help and piloting of the aircraft. We thank Professor Conglai Shen for developing the sample inlets, and Jiefang Yang for his operation on board. We also thank NASA for providing the OMI retrievals and Drs. N.A. Krotkov and X.L. Wei for their help in satellite data analysis. This work was funded by the National Basic Research Program (973 Program) of China (2005CB422203) and the Hong Kong Polytechnic University (1-BB94). We thank the two anonymous reviewers for their suggestions which have helped improve the original manuscript.

References

- Ahn, C., Torres, O., Bhartia, P.K., 2008. Comparison of ozone monitoring instrument UV aerosol products with Aqua/Moderate resolution imaging spectroradiometer and multiangle imaging spectroradiometer observations in 2006. *J. Geophys. Res.* 113, D16S27. doi:10.1029/2007JD008832.
- Carn, S.A., Krueger, A.J., Krotkov, N.A., Yang, K., Levelt, P.F., 2007. Sulfur dioxide emissions from Peruvian copper smelters detected by the Ozone Monitoring Instrument. *Geophys. Res. Lett.* 34, L09801. doi:10.1029/2006GL029020.
- Chan, C.K., Yao, X., 2008. Air pollution in mega cities in China. *Atmos. Environ.* 42, 1–42.
- Colarco, P.R., Toon, O.B., Torres, O., Rasch, P.J., 2002. Determining the UV imaginary index of refraction of Saharan dust particles from TOMS data using a three-dimensional model of dust transport. *J. Geophys. Res.* 107 (D16), 4289.
- Dickerson, R.R., et al., 2007. Aircraft observations of dust and pollutants over northeast China: insight into the meteorological mechanisms of transport. *J. Geophys. Res.* 112, D24S90. doi:10.1029/2007JD008999.
- Ding, A.J., et al., 2009. Transport of north China air pollution by mid-latitude cyclones: case study of aircraft measurements in summer 2007. *J. Geophys. Res.* 114, D08304. doi:10.1029/2008JD011023.
- Guibert, S., Matthias, V., Schulz, M., Bosenberg, J., Eixmann, R., Mattis, I., Pappalardo, G., Perrone, M.R., Spinelli, N., Vaughan, G., 2005. The vertical distribution of aerosol over Europe: synthesis of one year of EARLINET aerosol lidar measurements and aerosol transport modeling with LMDzT-INCA. *Atmos. Environ.* 39, 2933–2943.
- Hains, J.C., Taubman, B.F., Thompson, A.M., Stehr, J.W., Marufu, L.T., Doddridge, B.G., Dickerson, R.R., 2008. Origins of chemical pollution derived from mid-Atlantic aircraft profiles using a clustering technique. *Atmos. Environ.* 42, 1727–1741.
- Hao, J.M., Wang, L.T., 2005. Improving urban air quality in China: Beijing case study. *J. Air Waste Manag. Assoc.* 55, 1298–1305.
- IPCC, 2007. Climate change. In: Solomon, S., Qin, D., Manning, M., Chen, Z., Marquis, M., Avery, K.B., Tignor, M., Miller, H.L. (Eds.), *The Physical Scientific Basis. Contribution of Working Group I to the Fourth Assessment Report of the Intergovernmental Panel on Climate Change*. Cambridge University Press, Cambridge, United Kingdom, and New York NY, USA, 2007.
- Krotkov, N.A., et al., 2008. Validation of SO₂ retrievals from the ozone Monitoring instrument (OMI) over NE China. *J. Geophys. Res.* 113, D16S40. doi:10.1029/2007JD008818.
- Krotkov, N.A., Carn, S.A., Krueger, A.J., Bhartia, P.K., Yang, K., 2006. Band residual difference algorithm for retrieval of SO₂ from the Aura Ozone Monitoring Instrument (OMI). *IEEE Trans. Geosci. Remote Sens.* 44 (5), 1259–1266.
- Li, Y., Oberheitmann, A., 2009. Challenges of rapid economic growth in China: reconciling sustainable energy use, environmental stewardship and social development. *Energy Policy* 37, 1412–1422.
- Likens, G.E., Bormann, F.H., Johnson, N.M., 1972. Acid rain. *Environment* 14 (2), 33–40.
- Malm, W.C., Day, D.E., 2001. Estimates of aerosol species scattering characteristics as a function of relative humidity. *Atmos. Environ.* 35, 2845–2860.
- Ohara, T., Akimoto, H., Kurokawa, J., Horii, N., Yamaji, K., Yan, X., Hayasaka, T., 2007. An Asian emission inventory of anthropogenic emission sources for the period 1980–2020. *Atmos. Chem. Phys.* 7, 4419–4444.
- Pathak, R.K., Wu, W.S., Wang, T., 2009. Summertime PM_{2.5} ionic species in four major cities of China: nitrate formation in an ammonia-deficient atmosphere. *Atmos. Chem. Phys.* 9, 1711–1722.
- Penner, J.E., Chuang, C.C., Grant, K., 1998. Climate forcing by carbonaceous and sulfate aerosols. *Clim. Dyn.* 14 (12), 839–851.
- Preunkert, S., Legrand, M., Jourdain, B., Dombrowski-Etchevers, I., 2007. Acidic gases (HCOOH, CH₃COOH, HNO₃, HCl, and SO₂) and related aerosol species at a high mountain Alpine site (4360 m elevation) in Europe. *J. Geophys. Res.* 112, D23S12. doi:10.1029/2006JD008225.
- Seinfeld, J.H., Pandis, S.N., 2006. *Atmospheric Chemistry and Physics: From Air Pollution to Climate Change*. Wiley, New York, NY.
- Smith, S.J., Pitcher, H., Wigley, T.M.L., 2001. Global and regional anthropogenic sulfur dioxide emissions. *Glob. Planetary Change* 29, 99–119.
- Torres, O., et al., 2007. Aerosols and surface UV products from Ozone Monitoring Instrument observations: an overview. *J. Geophys. Res.* 112, D24S47. doi:10.1029/2007JD008809.
- Vestreng, V., Myhre, G., Fagerli, H., Reis, S., Tarrason, L., 2007. Twenty-five years of continuous sulphur dioxide emission reduction in Europe. *Atmos. Chem. Phys.* 7, 3663–3681.
- Wang, Wei, Liu, Hongjie, Yue, Xin, Li, Hong, Chen, Jianhua, Tang, Dagang, 2005. Study on size distributions of airborne particles by aircraft observation in spring over eastern coastal areas of China. *Adv. Atmos. Sci.* 22, 328–336.
- Wang, W.X., Wang, T., 1996. On acid rain formation in China. *Atmos. Environ.* 30, 4095–4099.
- Ware, J.H., Tribodeau, L.A., Speizer, F.E., Colome, S., Ferris, B.G., 1981. Assessment of the health effects of atmospheric sulfur oxides and particulate matter: evidence from observational studies. *Environ. Health Perspect.* 42, 255–276.
- Wild, O., Akimoto, H., 2001. Intercontinental transport of ozone and its precursors in a three-dimensional global CTM. *J. Geophys. Res.* 106 (D21), 27729–27744.
- Xu, Y.W., Carmichael, G.R., 1998. Modeling the dry deposition velocity of sulfur dioxide and sulfate in Asia. *J. Appl. Meteor.* 37, 1084–1099.